Flow around a Sphere in a Circular Tube

W. R. SMYTHE
California Institute of Technology, Pasadena, California
(Received January 6, 1961)

The vector potential for the flow of an ideal fluid through a tube containing a concentric spherical obstacle is found for ratios of sphere radius to tube radius of 0.1, 0.2, 0.3, 0.4, 0.5, 0.6, 0.7, 0.8, 0.9, and 0.95. The flow is confined to the space between sphere and cylinder by thin vortex sheets of variable strength and a table of their circulation intensity on the spherical surface is given. Accuracies vary from about one part in 10^8 for small spheres to one part in 10^7 for large ones. The increase in the scalar velocity potential between the ends of the tube caused by the insertion of the sphere is expressed in terms of the effective increase in tube length. This also gives the increase in resistance of a solid conducting cylinder due to the presence of a concentric spherical bubble.

I. INTRODUCTION

THE flow around a spherical obstacle in a circular tube cannot be solved by the usual method of separation of variables because the boundaries do not fit any separable orthogonal coordinate system. The solutions of analogous electrical problems[1,2] suggest superposition on the uniform flow system of that shown in Fig. 1(b). Here one set of coaxial closed vortex filaments[3,4] covers the sphere and an opposed set the cylinder. The filament density distribution is continuous and such that the flow is uniform inside the sphere and bounded by the cylinder. With axial symmetry and no sources, the vector velocity potential[3,4] has only one component A_ϕ and is zero both at $\rho = 0$ and $\rho = a$ because the net flow through any cylinder section, given by $\oint \mathbf{A}\cdot d\mathbf{s}$ around it, is zero. Furthermore, the vector velocity potential generated by a vortex filament whose strength is defined by the circulation k around it is the same as the magnetic vector potential in mks units produced by an electric line current i of identical shape if k is replaced by μi, where μ is the permeability. Thus electromagnetic formulas for the latter may be used here, with this substitution.

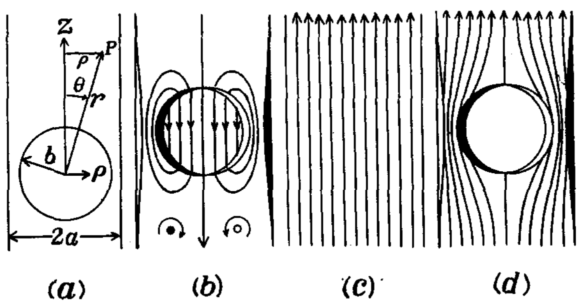

FIG. 1. (a) Coordinates systems. (b) Schematic diagram showing location of vortex sheets on surface of sphere and cylinder with clockwise circulation solid and counterclockwise open and the qualitative behavior of the lines of flow. (c) Uniform flow pattern. (d) Superposition of (b) and (c).

II. METHOD OF SOLUTION

The uniform velocity v_0 far from the sphere has only a z component and derives from the vector potential

$$A'_\phi = -\tfrac{1}{2}v_0\rho. \quad (1)$$

The circulation density assumed on the surface of the sphere is

$$k_\phi = v_0 \sum_{n=1}^{N} C_n P^1_{2n+1}(\cos\theta). \quad (2)$$

The vector potential of these vortices is[5]

$$r < b \qquad A_\phi = \sum_{n=1}^{N} \frac{bv_0C_n}{4n+3}\left(\frac{r}{b}\right)^{2n+1} P^1_{2n+1}(\cos\theta) \quad (3)$$

$$r > b \qquad A_\phi = \sum_{n=1}^{N} \frac{bv_0C_n}{4n+3}\left(\frac{b}{r}\right)^{2n+2} P^1_{2n+1}(\cos\theta). \quad (4)$$

[1] W. R. Smythe, J. Appl. Phys. **31**, 553 (1960).

[2] T. T. Taylor, J. Research Natl. Bur. Standards **64B**, 199 (1960). Here the flow around a short right circular solid cylinder at any angle is calculated by the superposition on a uniform flow of a suitable distribution of current or vortex filaments on the cylinder. For transverse flow the filament shapes are very complicated and all components of the vector potential are present so it is simpler to use the scalar potential generated by a double layer, one layer consisting of sources and the other of sinks but with identical distributions and very close together. This layer is termed a magnetic shell in electromagnetic theory and the scalar potential is discontinuous across it. A paper yet to be published will give the practical applications of these results.

[3] L. M. Milne-Thompson, *Theoretical Hydrodynamics* (The MacMillan Company, New York, 1955), 3rd ed., Ch. XVIII and especially article 18.24 and problem 2.

[4] A. Sommerfeld, *Mechanics of Deformable Bodies* (Academic Press, Inc., New York, 1950), Article 20.

[5] W. R. Smythe, *Static and Dynamic Electricity* (McGraw-Hill Book Company, Inc., New York, 1960), p. 273.

A formula relating spherical and cylindrical systems is

$$\frac{P^1_{2n+1}(\cos\theta)}{r^{2n+2}} = \frac{2(-1)^n}{\pi(2n)!}\int_0^\infty t^{2n+1}K_1(t\rho)\cos tz\,dt, \qquad (5)$$

so that the vector potential of the wall vortices required to cancel that of the sphere at $\rho = a$ is

$$\sum_{n=1}^{N}\frac{(-1)^{n+1}2v_0C_nb^{2n+3}}{\pi(4n+3)(2n)!}\int_0^\infty \frac{t^{2n+1}K_1(ta)I_1(t\rho)\cos tz}{I_1(ta)}\,dt. \qquad (6)$$

At $z = 0$ or $\theta = \frac{1}{2}\pi$ the first power of ρ in the sum of (3) and (6) must cancel (1) and the coefficients of the higher powers must vanish so that (1) is canceled throughout the volume of the sphere. When $I_1(t\rho)$ is expanded in powers of ρ at $z = 0$, the infinite integral appears in a form which may be integrated by parts, thus

$$(2s+1)\int_0^\infty \frac{(at)^{2s}K_1(at)\,d(at)}{I_1(at)} = \int_0^\infty \frac{x^{2s}\,dx}{I_1^2(x)} = I(2s). \qquad (7)$$

This integral, which appears in subsequent calculations, was evaluated numerically using Weddles rule and intervals of 0.1. The results, which appear in Table I, are uncertain in the last digit due to rounding off errors.

Equating the ρ^p coefficients to zero when $1 < p < N + 1$ on the assumption that C_n is negligible when $n > N$ gives $N + 1$ simultaneous linear equations for C_n. Thus

$$\frac{\delta_p^2}{2} = \frac{2(4p+3)q^3}{3\pi(2p+2)!}\cdot\sum_{n=0}^{N}\frac{(-q^2)^{n+p}C_nI(2n+2p+2)}{(4n+3)(2n+2p+3)(2n)!} - \frac{C_p}{3}, \qquad (8)$$

where $q = b/a$ and δ_p^0 is zero if $p \neq 0$ and one if $p = 0$. These equations were solved for C_n for b/a values of 0.1, 0.2, 0.3, 0.4, 0.5, 0.6, 0.7, 0.8, 0.9, and 0.95 with the results shown in Table II. None of the digits included change when N is increased so all digits given should be significant.

TABLE I. Values of $(s!)^{-2}I(2s) = (s!)^{-2}\int_0^\infty t^{2s}I_1(t)^{-2}\,dt$.

n	$(n!)^{-2}I(2n)$	n	$(n!)^{-2}I(2n)$	n	$(n!)^{-2}I(2n)$
0	∞	14	7.1837361	28	9.7621311
1	7.5060642	15	7.3964574	29	9.9212532
2	4.7120880	16	7.6035858	30	10.077895
3	4.5554925	17	7.8055005	31	10.232169
4	4.7231790	18	8.0025468	32	10.384177
5	4.9698807	19	8.1950391	33	10.534015
6	5.2362852	20	8.3832624	34	10.681772
7	5.5038276	21	8.5674759	35	10.827531
8	5.7661524	22	8.7479154	36	10.971371
9	6.0211500	23	8.9247957	37	11.113364
10	6.2683098	24	9.0983130	38	11.253580
11	6.5077497	25	9.2686470	39	11.392082
12	6.7398339	26	9.4359624	40	11.528932
13	6.9650091	27	9.6004107	41	11.664189

TABLE II. Vortex density coefficients C_n.

n	$b = 0.1a$
0	−1.5011956
1	0.0000035025
2	−0.0000000114
3	0.00000000003

n	$b = 0.2a$
0	−1.5096182
1	0.0001127114
2	−0.0000014677
3	0.0000000184
4	−0.0000000002

n	$b = 0.3a$
0	−1.5329642
1	0.0008691944
2	−0.0000254684
3	0.0000007202
4	−0.0000000196
5	0.0000000005

n	$b = 0.4a$
0	−1.5805729
1	0.0037782088
2	−0.0001969050
3	0.0000099055
4	−0.0000004805
5	0.0000000227
6	−0.0000000010

n	$b = 0.5a$
0	−1.6659472
1	0.012176732
2	−0.009936887
3	0.000783265
4	−0.000059578
5	0.000004407
6	−0.000000319
7	0.000000023
8	−0.000000002

n	$b = 0.6a$
0	−1.8124644
1	0.033180471
2	−0.003927532
3	0.000450142
4	−0.000049919
5	0.000005400
6	−0.000000574
7	0.000000060
8	−0.0000000063
9	0.0000000006

n	$b = 0.7a$
0	−2.0688531
1	0.083384154
2	−0.013717061
3	0.002200950
4	−0.000344491
5	0.000053071
6	−0.000008111
7	0.000001237
8	−0.000000189
9	0.000000029
10	−0.0000000045
11	0.0000000007

n	$b = 0.8a$
0	−2.5643499
1	0.21130158
2	−0.047912301
3	0.010792575
4	−0.002416781
5	0.000542599
6	−0.000122889
7	0.000028162
8	−0.000006534
9	0.000001534
10	−0.000000364
11	0.000000087
12	−0.000000021
13	0.0000000050
14	−0.0000000012
15	0.0000000003

n	$b = 0.9a$
0	−3.8319456
1	0.64394874
2	−0.21166126
3	0.071636583
4	−0.024790489
5	0.008763604
6	−0.003155347
7	0.001152676
8	−0.000425616
9	0.000158389
10	−0.000059282
11	0.000022277
12	−0.000008405
13	0.000003179
14	−0.000001205
15	0.000000458
16	−0.000000174
17	0.000000067
18	−0.000000025
19	0.000000010

n	$b = 0.95a$
0	−5.7826704
1	1.4673995
2	−0.62160624
3	0.27772236
4	−0.12838477
5	0.060838137
6	−0.029343698
7	0.014331470
8	−0.007063127
9	0.003504745
10	−0.001748364
11	0.000869671
12	−0.000440486
13	0.000222186
14	−0.000112373
15	0.000056966
16	−0.000028937
17	0.000014724
18	−0.000007504
19	0.000003829
20	−0.00000196

III. POTENTIAL

The vector potential between sphere and cylinder is the sum of (1), (4), and (6). The calculation of the integral in (6) is aided by the expansion of $I_1(t\rho)$ in powers of ρ and of $\cos tz$ in powers of z which give

$$\sum_{s=0}^{\infty}\sum_{r=0}^{\infty}\frac{(-1)^r(\frac{1}{2}\rho)^{2s+1}z^{2r}I(2n+2r+2s+2)}{s!(s+1)!(2r)!(2n+2r+2s+3)a^{2n+2r+2s+3}}. \qquad (9)$$

This becomes a single summation on the axis where ρ is zero and in the equatorial plane where z is zero.

TABLE III. Bessel function expansion coefficients $D_r(b/a)$.

r	$D_r(0.1)$	$D_r(0.2)$	$D_r(0.3)$	$D_r(0.4)$	$D_r(0.5)$
1	−0.00616957	−0.049633	−0.170076	−0.415233	−0.850990
2	−0.0111114	−0.089387	−0.306193	−0.745776	−1.513194
3	−0.0160506	−0.129117	−0.442044	−1.072794	−2.145897
4	−0.0209895	−0.168839	−0.577614	−1.395341	−2.744941
5	−0.0259283	−0.208554	−0.712837	−1.712727	−3.313170
6	−0.0308670	−0.248261	−0.847655	−2.024706	−3.860297
7	−0.0358057	−0.287959	−0.982016	−2.331511	−4.401127
8	−0.0407444	−0.327647	−1.115883	−2.633848	−4.952673
9	−0.0456831	−0.367323	−1.249232	−2.932846	−5.530711
10	−0.0506218	−0.406986	−1.382054	−3.229968	−6.14644
11	−0.0555604	−0.446635	−1.514354	−3.52689	−6.80390
12	−0.0604991	−0.486269	−1.646154	−3.82538	−7.4986
13	−0.0654377	−0.525887	−1.777488	−4.1271	−8.2182
14	−0.0703762	−0.565488	−1.908405	−4.4336	−8.944
15	−0.0753149	−0.605071	−2.038968	−4.7460	−9.653
16	−0.0802534	−0.644636	−2.169248	−5.0648	−10.32
17	−0.0851919	−0.684182	−2.299328	−5.390	−10.9
18	−0.0901304	−0.723709	−2.429296	−5.722	−11.
19	−0.0950689	−0.763216	−2.55925	−6.06	−12.
20	−0.1000074	−0.802702	−2.68928	−6.39	...

r	$D_r(0.6)$	$D_r(0.7)$	$D_r(0.8)$	$D_r(0.9)$	$D_r(0.95)$
1	−1.576673	−2.746212	−4.596724	−7.488546	−9.48391
2	−2.717612	−4.367863	−6.038241	−5.983745	−3.92018
3	−3.702970	−5.472225	−6.800447	−9.004879	−14.43542
4	−4.562687	−6.522897	−9.402522	−18.516958	−24.01881
5	−5.385117	−8.077419	−14.147385	−22.78879	−21.51984
6	−6.282479	−10.351228	−18.44602	−20.02176	−78.21
7	−7.344023	−13.00718	−19.81021	−21.230	−(>1000)
8	−8.595792	−15.34512	−18.987	−38.1	...
9	−9.98364	−16.784	−19.4	−171.	
10	−11.388	−17.31	−23.		
11	−12.66	−17.6			
12	−13.7	−18.			
13	−14.5				
14	−15				

The ρ summation always converges rapidly but the z summation only when z is much less than a.

Another expansion that is useful when z is large is

$$A_\phi = v_0\left[\tfrac{1}{2}\rho + \sum_{r=1}^{\infty} D_r J_1(k_r\rho)e^{-k_r z}\right], \qquad (10)$$

where k_r is chosen so that $J_1(k_r a) = 0$ and

$$D_r = \frac{2b^3}{a^2 J_0^2(k_r a)} \sum_{n=0}^{N} \frac{(k_r b)^{2n} C_n}{(4n+3)(2n)!}. \qquad (11)$$

Values of D_r for each b/a are given in Table III.

The equation of the stream function ψ is

$$\psi = 2\pi\rho A_\phi. \qquad (12)$$

IV. ACCURACY

A numerical check was made by the calculation of A_ϕ at the equator, where it should be zero using (1), (4), (6), and (9). The results in the first column of Table IV show a decrease in accuracy as b approaches a. In this case the sphere and wall terms nearly cancel so the difference error is large. At the pole of the sphere A_ϕ vanishes in all formulas so the check must be made on v_z which should also vanish. The results, using (1), (4), (6), and (9) in the second column of Table IV, are good except in the case of $b/a = 0.95$. The 0.95 check would be much closer if Table I were extended to higher n values. The last column of the table gives some pole checks on v_z using (10) and (11). It shows the limitations of these formulas in finding **v**. The

TABLE IV. Numerical checks.

b/a	A_ϕ at equator [(1), (4), (6), (9)]	v_z at pole [(1), (4), (6), (9)]	v_z at pole [(10) and (11)]
0.1	−0.0000000009	+0.00000002	...
0.2	−0.0000000016	+0.00000008	...
0.3	−0.000000013	−0.00000002	...
0.4	−0.000000018	+0.00000003	...
0.5	−0.000000021	+0.00000001	−0.000047
0.6	−0.000000017	+0.00000004	−0.000082
0.7	+0.00000001	−0.00000002	−0.000132
0.8	−0.00000003	−0.00000012	−0.000218
0.9	+0.00000005	−0.00000006	−0.000401
0.95	+0.0000001	+0.0000478	−0.000640

curl of (10) always converges for z greater than zero because of the exponential factor but it appears that beyond the range of Table III D_r becomes large enough to make significant contributions to $\mathbf{v}$. The last D_r in this table is certainly over a thousand. The A_ϕ values from (10) should be much better. The last digit given for C_n in Table II is significant in most cases.

V. EFFECTIVE INCREASE IN LENGTH OF TUBE

The insertion of the sphere between two points in the tube sufficiently far apart will leave the flow at these points unperturbed but will increase the scalar velocity potential difference between them. The same change would result with no sphere if the distance between the points were increased by an amount ΔL. This quantity is found by taking the line integral, divided by v_0, of that part of $\mathbf{v}$ produced by sphere and wall vortices along a path between sphere and cylinder from $z = -\infty$ to $z = +\infty$. The sphere vortices contribute nothing. The wall contribution is found by taking the z component of the curl of (6). This replaces $I_1(t\rho)$ by $I_0(t\rho)$ and increases the power of t by one. The value of the integrand is then $2a^{-3}$ when $n = 0$ and zero when $n \neq 0$ so that, by Fourier's integral theorem, the z integration replaces the integral by $2\pi a^{-3}$. Thus the effective increase in length is

$$\Delta L = v_0^{-1} \int_{-\infty}^{+\infty} v_z \, dz = 4(b/a)^3 C_0. \tag{13}$$

The values of C_0 appear in Table II. This also gives the increase in resistance of a solid conducting cylinder due to the presence of a concentric insulating sphere or bubble inside it.

THE PHYSICS OF FLUIDS VOLUME 4, NUMBER 6 JUNE, 1961

Generalizations of the Saha Equation

EDMOND M. DEWAN*
Air Force Cambridge Research Laboratories, Bedford, Massachusetts
(Received August 10, 1960; revised manuscript received February 23, 1961)

The Saha equation, which relates temperature to ion densities, is sometimes used under circumstances that do not justify the assumptions of thermodynamic equilibrium upon which it is based. Astronomers have therefore made generalizations of this equation but have unfortunately assumed thermodynamic equilibrium energy distributions for the particles and the radiation field even though these may be at different temperatures. It is therefore interesting to know how the nonequilibrium *steady-state* energy distributions affect the ionization densities. In the present treatment a general expression relating ion densities to the radiation and particle energy distributions is obtained. This equation reduces to Saha's equation in the limit of thermal equilibrium and gives numerical results in good agreement with other work based on entirely different considerations, thus providing a good check. We find that under certain conditions one would expect results that differ *enormously* from those predicted by the Saha equation.

I. INTRODUCTION

THE first investigations of the temperature dependence of the densities of atoms ionized to various degrees in a plasma (hereafter referred to as various "stage" ions) were carried out by Saha[1] and Eggert.[2] Their equation (below) assumes thermodynamic equilibrium, a condition not fulfilled in many cases of physical interest.

$$\frac{n_{j+1}n_e}{n_j} = \frac{\tilde{\omega}_{j+1}}{\tilde{\omega}_j} \frac{2(2\pi m\kappa T)^{\frac{3}{2}}}{h^3} e^{-\epsilon_j/\kappa T}, \tag{1}$$

where n_j is the number of jth-stage ions and n_e the number of free electrons per cubic centimeter, m is the mass of an electron, κ and h Boltzmann's and Planck's constants, respectively, $\tilde{\omega}_j$ is the partition function for jth-stage ion[3] ϵ_j is the ionization potential of the jth-stage ion, and T is the temperature.

This equation is often used to obtain plasma temperatures from spectral-line information. Since

* Based on a thesis submitted in partial fulfillment of the requirements for the degree of Doctor of Philosophy at Yale University.

[1] M. N. Saha, Phil. Mag. **40**, 472 (1920); Z. Physik **6**, 40 (1921).

[2] J. Eggert, Physik Z. **20**, 570 (1919).

[3] Values can be found in R. H. Fowler, *Statistical Mechanics* (Cambridge University Press, Cambridge, England, 1936), 2nd ed., p. 569.